

1 SHORT COMMUNICATION

2
3 **Influence of the scanned side of the row in terrestrial laser sensor applications in**
4 **vineyards: practical consequences**

5
6 **Jaume Arnó · Alexandre Escolà · Joan Masip · Joan R. Rosell-Polo**
7

8
9
10
11 J. Arnó (✉) · A. Escolà · J. Masip · J. R. Rosell-Polo

12 Department of Agricultural and Forest Engineering, Research Group on AgroICT and
13 Precision Agriculture, University of Lleida, Rovira Roure, 191, 25198 Lleida, Spain

14 e-mail: JArno@eagrof.udl.cat

15 URL: www.grap.udl.cat
16
17
18
19
20

21 **Abstract** Terrestrial laser scanners (TLS) have been used to estimate leaf area and
22 optimise the site-specific management in vineyards. The tree area index (TAI) is a
23 parameter that can be obtained from TLS measurements and has been highly successful
24 in predicting the leaf area index (LAI) in vineyards using linear regression models.
25 However, there are concerns about the possible variation of the models according to the
26 row side on which the scan is performed. A field trial was performed in a North-South
27 oriented vineyard using a tractor-mounted LiDAR system to determine the influence of
28 this operational factor. Four vineyard blocks were scanned from both sides and then
29 defoliated to obtain the real LAI values for 1-m row length sections. Specifically, LAI
30 values were obtained considering the total canopy width and, after separation of the
31 leaves of the right and left sides, LAI values of half canopy were also calculated. To
32 estimate the LAI from the TAI, dummy-variable regression models were used which
33 showed no differences with respect to the scanned side of the canopy. Two
34 consequences are immediate. First, TLS made it possible the LAI mapping of two
35 different rows by scanning from the alley-way with an appropriate laser scanner.

36 Secondly, the same model can be used to estimate the LAI of half canopy (right or left)
37 in operations that require going through all inter-rows (e.g., when applying plant
38 protection products in a vineyard to estimate the vegetation exposed to the sprayer).

39

40 **Keywords** LiDAR · Ground-based laser sensor · TAI · LAI · Dummy-variable
41 regression

42

43 **Introduction**

44 The use of sensors in viticulture is already known and accepted. Among their
45 applications, canopy characterisation has been the focus of much of the research, and
46 the estimation of leaf area or leaf area index (LAI) remains a clear objective of the
47 studies published to date (Jonckheere et al. 2004). The technologies used are also
48 different, with ultrasonic sensors, plant canopy analysers (ceptometers), and radiometric
49 devices widely studied (Goutouly et al. 2006; Johnson and Pierce 2004; Llorens et al.
50 2011). In the latter case, differences between the use of satellite, airborne, and ground-
51 based sensors have been highlighted. However, all these technologies have some
52 constraints. It is known, for example, that vegetation indices derived from remote
53 sensing typically require a specific calibration according to the different growth stages
54 of the vines (Johnson et al. 2003). The presence of soil and/or weeds between rows also
55 complicates the correct interpretation of reflectance data in the images. Additionally, the
56 cost of the images is not always affordable for small and medium-size winegrowers.
57 Compared to remote sensors, ground-based radiometric sensors have also been
58 referenced by several authors (Drissi et al. 2009; Mazzetto et al. 2010; Stamatiadis et al.
59 2010). Although their operation avoids the previously mentioned problems, their
60 drawback is probably the difficulty in covering the total height of vine vegetation and,

61 consequently, in obtaining a reliable reflectance measurement of the total canopy
62 volume.

63

64 Ultrasonic sensors have also been successfully applied in viticulture. In this case,
65 problems are related to their low vertical sampling resolution, which does not allow a
66 detailed measurement of the canopy unless a sensor array is implemented (Lee and
67 Ehsani 2009). Both radiometric and ultrasonic sensors enable continuous evaluation of
68 the canopy along the row. This feature is currently impossible for ceptometers and
69 similar optical instruments, which also tend to significantly underestimate the LAI
70 (Johnson and Pierce 2004).

71

72 In recent years, interest in laser sensors, as well as new applications of light
73 detection and ranging (LiDAR) technologies in agriculture, has greatly increased.
74 Experiments in vineyards have been referenced, among others, by Rosell et al. (2009),
75 López-Lozano et al. (2009), and Llorens et al. (2011). Specifically, given their higher
76 resolution, better adaptation to the crop, and possible on-the-go use, laser scanners have
77 been used to estimate LAI and canopy density. More recently, Arnó et al. (2013)
78 developed an algorithm to calculate the tree area index (TAI) from data supplied by
79 terrestrial laser scanners (TLS). The LAI is then estimated through the TAI using linear
80 regression models.

81

82 In relation to this procedure, TLS are used laterally either from the right or from
83 the left of the row, thus there may be some doubts whether the same model can be
84 applied to estimate the LAI from TAI regardless of the scanned side of the canopy.
85 Previous works propose estimating the LAI from LiDAR data using together the scans

86 performed on both sides of the row (Rosell et al. 2009; Sanz et al. 2011). This implies a
87 more complex management of LiDAR data and, in any case, complicates the estimation
88 of the leaf area index on-the-go. Additionally, these systems increase the operation
89 costs. Faced with this approach, Arnó et al. (2013) propose using the LiDAR from one
90 side of the row but without specifying the right or left side. However, the potential
91 influence of the orientation of the rows in the differential growth in both sides of the
92 vines makes it necessary to study whether the scanned side significantly influences the
93 result of the estimation. Moreover, it is not clear whether this approach is also
94 applicable to the estimation of the LAI of only half the row width. This is especially
95 relevant in plant protection product applications in which the sprayer travels along all
96 the alley-ways, as it is necessary to estimate the vegetation exposed to the sprayer. Since
97 dose adjustment to the canopy is crucial to improve the efficiency of applications (Gil et
98 al. 2007; Llorens et al. 2011), LAI estimation for half canopy for two adjacent rows is
99 necessary and makes sense to the use of a single model that only considers this partial
100 vegetation.

101

102 The main objective of this communication was to study the influence of the
103 scanned side of the canopy on the effectiveness of TLS to estimate LAI in vineyards.
104 This work is focused on the estimation of the LAI in *Vitis vinifera* L. cv. Merlot and
105 complements the results obtained by Arnó et al. (2013). As the scanned side was the
106 factor under analysis, dummy-variable regression was used to compare and evaluate the
107 regression models and their structural stability. This regression analysis procedure is
108 explained in more detail in the following paragraphs.

109

110 **Materials and methods**

111 Terrestrial laser scanner (TLS)

112 The TLS (or LiDAR sensor) used in this study was the LMS-200 model (SICK AG,
113 Waldkirch, Germany). More detailed information can be found in Arnó et al. (2013). As
114 a basic feature, the sensor operation is based on the time-of-flight (TOF) principle to
115 estimate the distance to the canopy. A two-dimensional fan-shaped scan is obtained
116 because the beam is pulsed with an angular resolution of 1° in the vertical cross-
117 sectional plane. Thus, by scanning the vines from one side of the row, the sensor
118 provides the polar coordinates of each interception point, i.e., the radial distance and the
119 angle of the laser beam. When the laser sensor is mounted on a moving tractor, multiple
120 vertical scans along the row can be obtained. Table 1 lists the configuration and
121 operation settings used in the field test. Data transfer from the sensor to a laptop was
122 done via the RS-232 protocol using a MATLAB-based program for sensor control and
123 data acquisition. This same software was used to process the information and obtain the
124 tree area index (TAI) parameter.

125

126 **Table 1** SICK LMS-200 configuration and operation settings

Maximum measurement distance (m)	8
Accuracy (mm)	±15
Angular resolution (°)	1
Scanning angular range (°)	180
Scanning sampling frequency (scans s ⁻¹)	12
Horizontal scanning resolution or distance between scans (cm)	2.3
Travel speed (km h ⁻¹)	1

127

128 Tree area index measurement

129 The process for obtaining the TAI is explained in detail in Walklate et al. (2002), and
130 was later adapted for use in a vineyard by Arnó et al. (2013) as shown in Figure 1. The
131 tractor-mounted LiDAR sensor was moving in the direction of the Oz axis (not shown)
132 parallel to the ground. Several scans were obtained along the row in different vertical
133 planes parallel to plane Oxy . Finally, all interception points within the canopy were

134 projected relative to the Oz axis onto a two-dimensional grid of polar cells in the Oxy
 135 plane (Fig. 1). In particular, the overall projected cross-section of the canopy volume
 136 was divided into cells with equal angular increments of $\Delta\theta = 3^\circ$ and equal radial
 137 increments of $\Delta r = 100$ mm. For each (k -th, j -th) cell, it was possible to calculate the
 138 number of laser beams reaching the input side of the polar cell, $n_{k,j}$, and the number of
 139 interceptions, $\Delta n_{k,j}$, within the cell. The TAI was finally calculated using equation [1]

$$140 \quad TAI = -\frac{\Delta\theta}{W} \sum_{k=1}^K \sum_{j=1}^{J_k} r_j \delta_{k,j} \ln\left(1 - \frac{\Delta n_{k,j}}{n_{k,j}}\right) \quad (1)$$

141 where, apart from the abovementioned $\Delta\theta$, $\Delta n_{k,j}$, and $n_{k,j}$, W (m) is the distance
 142 between vine rows, r_j (m) is the radial distance between the polar cell and the sensor
 143 position, and $\delta_{k,j}$ is a function that detects the presence or absence of foliage in each cell
 144 ($\delta_{k,j} = 1$ when the coefficient $\Delta n_{k,j} / n_{k,j}$ is greater or equal to 0.01, and $\delta_{k,j} = 0$ when the
 145 coefficient is less than 0.01). In practical terms, the TAI obtained from equation [1] is
 146 formulated as the ratio between the crop area detected by the TLS and the ground area.
 147 In the calculation of the TAI, it is also assumed that the probability of the laser beam
 148 transmission within vines can be approximated by the Poisson probability model when
 149 sufficiently small distances (Δr) and random spatial distribution of the leaves are
 150 considered.

151

152 **Fig. 1** Two-dimensional grid of polar cells to calculate the TAI (Arnó et al. 2013). Each
 153 polar cell is defined by two coordinates (r_j, θ_k). The first one, r_j , is the distance from the
 154 reference origin (LiDAR sensor), and the second one, θ_k , is the angle between the Oy
 155 axis and the radial direction (clockwise). H_g is the height of the LiDAR sensor
 156 measured from the ground (approximately constant, 1.60 m), and d_t is the distance used
 157 to exclude intercepted points at ground and trunk levels

158

159 Field trial

160 A field test was conducted on an experimental vineyard located in Raimat (Lleida,
161 Spain). Specifically, the vineyard chosen had a surface area of 16.92 ha and was planted
162 in 1998 with *Vitis vinifera* L. cv. Merlot using a pattern of 3 × 2 m. Vertical shoot
163 position (VSP) was used as a training system. The cordon height was 1.10 m, two
164 parallel wires were placed at 1.40 m, and a third wire was placed at 1.80 m. During the
165 measurements, the height of vines reached about 2.10 m at the stage of higher
166 vegetative growth. The vineyard was drip irrigated, and rows were oriented north-south
167 (N–S).

168

169 Four vineyard blocks at different locations within the study vineyard were
170 selected because field measurements were conducted at four different developmental
171 stages of the vines. According to BBCH-scale (Meier 2001), tests were performed
172 respectively in crop stages 17 (leaf development), 65 (flowering), 77 (development of
173 fruits) and 83 (ripening of berries). The used methodology was simple and can be
174 consulted in Arnó et al. 2013. Vineyard blocks were 4-m-long row sections
175 corresponding to the distance between three consecutive vine trunks. Once delimited,
176 four measurements were performed with the TLS (two from the left side and two from
177 the right side of the row) by moving the laser sensor along the row at a rate of about 1
178 km h⁻¹. Blocks were then manually completely defoliated by sections (vertical stripes)
179 of 1 m in length, differentiating the right side and the left side of the vine row using the
180 line of trunks as a reference. The objective was to obtain, for each block, the left LAI
181 and right LAI for the four 1-m sections. Subsequently, values of total LAI over the
182 entire row width for each 1-m long section were also obtained. Therefore, 12 LAI
183 measurements were performed for each block. A planimeter (Delta-T Devices Ltd.,
184 Cambridge, UK) was used to measure the surface area of a sample of leaves taken from

185 each of the defoliated blocks. The total leaf area was obtained by the gravimetric
186 method. In short, a sample of n leaves was taken from each of the blocks tested. The
187 leaf surface of this sample was measured, and the total surface area of each strip (right
188 or left side of 1 m in length) was finally obtained from the surface area-weight ratio of
189 the sample and the weight of all the leaves of the strip. In each case, the sample size n
190 was previously established using the expression [2]

$$191 \quad n = \frac{z_{\alpha/2}^2 \cdot CV^2}{E_R^2} \quad (2)$$

192 where E_R was the relative error assumed (10%), $z_{\alpha/2}$ the value of the standard normal
193 variate (SNV), and CV , the resulting value of leaf area variability (Coefficient of
194 Variation) of a pilot sample of 30 leaves.

195

196 The LiDAR sensor was always used before defoliating the vines. Therefore, TAI
197 values were obtained with the vineyard vegetation occupying the entire width of the
198 canopy. Then, an appropriate statistical analysis made it possible to assess the suitability
199 of a single model to estimate the LAI for the whole canopy and a different model to
200 estimate the LAI for only half of the canopy.

201

202 Statistical analysis

203 A linear regression analysis was performed to assess the suitability of the TAI
204 parameter for estimating LAI. However, models for estimating the LAI could differ,
205 depending on the scanning side used (i.e. scanning from the left side or from the right
206 side of the row). To determine this, the patterns obtained for both sides were compared
207 using dummy-variable regression. This statistical procedure allowed proposing the
208 following dummy-regression model with interactions,

209
$$Y_i = \alpha + \beta X_i + \gamma D_i + \delta(X_i D_i) + \varepsilon_i \quad (3)$$

210 where Y_i is the LAI, X_i is the quantitative regressor for the TAI, D_i is the dummy
 211 regressor for the ‘*scanning row side*’, coded ‘0’ for the right side and ‘1’ for the left
 212 side, and $X_i D_i$ is the interaction regressor between both the ‘*TAI*’ and the dichotomous
 213 explanatory variable ‘*scanning row side*’. The omitted category (right side) serves as a
 214 baseline against which the other category (left side) is compared. Therefore, the
 215 regression models used were in the following form,

216 Right side of the row ($D_i = 0$):
$$Y_i = \alpha + \beta X_i + \varepsilon_i \quad (4)$$

217 Left side of the row ($D_i = 1$):
$$Y_i = (\alpha + \gamma) + (\beta + \delta) X_i + \varepsilon_i \quad (5)$$

218

219 The proposed model is relevant because the dummy regressor (D_i) allows the
 220 incorporation of a new explanatory variable when there is reason to believe that the
 221 model coefficients are different between subsamples ‘right’ and ‘left’. Any structural
 222 change in the regression model was detected by the t -statistic, which was used
 223 individually to test the dummy and the interaction regressor coefficients. In our case [3],
 224 the contrasts were $H_0 : \delta = 0$, $H_a : \delta \neq 0$, for a difference in slope between ‘right side’
 225 and ‘left side’, and $H_0 : \gamma = 0$, $H_a : \gamma \neq 0$, for a difference in the intercept. Statistical
 226 analysis was performed using JMP® 10.0.0 (SAS Institute Inc.).

227

228 **Results**

229 The first analysis addressed the influence of the scanned side of the row on the
 230 estimation of the LAI for the entire canopy width (‘full LAI’) from the LiDAR. Two
 231 simple linear regression models were built from field data. The models were fitted to a
 232 basic structural expression in the form $LAI_i = \beta_0 + \beta_1 \cdot TAI_i + \varepsilon_i$, showing the linear

233 relationship between the LAI (dependent variable) and the TAI (explanatory variable)
 234 for left and right scanned row sides. Figure 2 shows the two models obtained. In both
 235 cases (scanning from the right side or from the left side), the TAI was able to explain a
 236 high percentage (~92%) of the variation in the leaf surface. This value can be
 237 considered satisfactory given the particular working difficulties in field conditions. As
 238 to the question whether the two models are significantly different, the statistical analysis
 239 (Table 2) confirmed that a single model can be used in both cases. In fact, Figure 2
 240 clearly shows that both regression lines are practically coincident. On the other hand,
 241 the regression coefficient of about 1.3 (disregarding the intercept) also confirms that
 242 TAI usually underestimates LAI because of the clumping effect normally observed in a
 243 vineyard.

244

245 **Table 2** Statistical analysis of dummy-regression models for LAI estimation in Merlot
 246 depending on the LiDAR scanning row side (left or right)

Model	Term	Estimate	Standard error	<i>t</i> ratio	<i>p</i> > <i>t</i>
Estimation of LAI of the total row width (1-m-long sections)					
LAI-right (baseline)	Intercept (α)	-0.2615	0.0827	-3.16	0.0025*
LAI-right (baseline)	X_i (β)	1.3275	0.0720	18.43	<0.0001*
LAI-left	D_i (γ)	0.0549	0.1148	0.48	0.6342
LAI-left	$X_i D_i$ (δ)	-0.0500	0.0998	-0.50	0.6179
Estimation of LAI for only half the row width (right or left sides, 1-m-long sections)					
LAI-right (baseline)	Intercept (α)	-0.3460	0.1199	-2.89	0.0054*
LAI-right (baseline)	X_i (β)	1.4540	0.1043	13.94	<0.0001*
LAI-left	D_i (γ)	0.1906	0.1664	1.15	0.2564
LAI-left	$X_i D_i$ (δ)	-0.2729	0.1446	-1.89	0.0639

247

248 The second analysis evaluated the LAI estimation by the TLS corresponding to
 249 half canopy width ('partial LAI'), i.e., the possibility of estimating the amount of
 250 vegetation between the trunk line and the outer surface of the foliage in which the laser
 251 sensor is projected. Regarding the differences between models (Fig. 2), there is a certain
 252 similarity of the lines, but the similarities are somewhat smaller than for the models for
 253 the 'full LAI', given the higher slope obtained when scanning the row from the right

254 side. However, statistical analysis (Table 2) again confirmed that the two models were
255 not significantly different.

256

257 **Fig. 2** Linear regression models of leaf area index (LAI) in a vineyard (*cv.* Merlot)
258 depending on the scanned side (left or right). The first column shows the models for the
259 ‘full LAI’ (32 points, 8 per block/vine growth stage), and the second column shows the
260 models for the ‘partial LAI’ (32 points, 8 per block/vine growth stage)

261

262 The interpretation of these results is interesting for two reasons. First, all
263 regression models must be formulated with a negative intercept. This is an expected
264 result because when the sensor is used in leafless vines (for example, in winter), LiDAR
265 readings also provide TAI values as the laser beam is intercepted by the wooden
266 structure of vines. Secondly, and more importantly, vines may be scanned easily and
267 efficiently by TLS either from the right or from the left side of the row to estimate the
268 full or partial LAI by applying the appropriate model in each case. Table 3 lists the
269 resulting regression analysis models.

270

271 **Table 3** Regression models to estimate the leaf area index (LAI) in a vineyard (*cv.*
272 Merlot) for 1-m row lengths

Type of LAI	Regression model
Entire row width (‘full LAI’)	$LAI = -0.26 + 1.33 \times TAI$
Half the row width (‘partial LAI’)	$LAI = -0.35 + 1.45 \times TAI$

273 TAI: Tree Area Index

274

275

276 Considering ‘full LAI’, the sensor can be used in an on-the-go manner for
277 mapping the LAI in vineyards with high spatial variability, and subsequently to define
278 zones of differential management. Using new commercially available LiDAR sensors
279 with detection angles of 270° (Fig. 3), the trajectory within the field is simplified, and
280 both data acquisition and post-processing are greatly improved by reducing the scanning

281 time and the amount of recorded data (LAI can be estimated reading only one side of
282 the row and the tractor scanning every other row). Another possibility is the use of
283 LiDAR sensors in combination with agricultural machinery, for example, when
284 applying plant protection products using variable-rate sprayers where continuous
285 monitoring of the LAI of each side of the row (or ‘partial LAI’) is needed. In this case
286 (Fig. 3), the system operation is again simplified because the same LAI estimation
287 model for both sides of the row can be adopted.

288

289 Finally, there is a factor linked to the parcel that may have some importance. In
290 our study, rows were oriented N–S. The question is whether the row orientation may
291 influence the use of TLS in vineyard and, in this regard, further investigations are
292 warranted. It is likely that in E-W oriented rows, there may be differences in the
293 exposure to sunlight experienced by the different sides of the row. In this case, it is not
294 clear that the same model could be applied to both sides, and additional data are needed
295 to corroborate or refute this hypothesis. For now, and for the analysed case, the models
296 (right side/left side) are consistent, which is an advantage for users, requiring less
297 computing resources in both acquisition and post-processing. Other non-operating
298 factors (such as grapevine cultivar and training system) should also be evaluated in
299 future research on the use of TLS in viticulture.

300

301 **Fig. 3** Trajectory described by a laser sensor to map the LAI (left), and operation of the
302 same sensor in combination with a sprayer for a variable rate application of plant
303 protection products (right). In the first case, the ‘full LAI’ estimation model could be
304 applied and, in the second, the ‘partial LAI’ model can be used

305

306

307 **Conclusions**

308 LAI can be estimated in vineyards with TLS using the TAI in appropriate linear
309 regression models. In rows oriented N–S, TLS can be applied for either side of the row,
310 and LAI estimation models only differ according to the main use of the sensor.
311 Specifically, mapping the ‘full LAI’ requires using a separate regression model to
312 estimate the leaf surface for the entire row width, making it possible to simplify the
313 scanner trajectory within the field. The model changes when estimating the ‘partial
314 LAI’, although it is equally applicable to both scanning sides. The advantages of both
315 applications lie in simplifying field use and reducing data acquisition and processing
316 time.

317

318 **Acknowledgements**

319 The authors acknowledge funding from the ERDF (European Regional Development
320 Fund) and the Spanish Ministry of Science and Education (OPTIDOSA research
321 project, AGL2007-66093-C04-03). Codorníu collaboration allowing the use of their
322 vineyards in Raimat is also greatly appreciated.

323

324 **References**

325 Arnó, J., Escolà, A., Vallès, J. M., Llorens, J., Sanz, R., Masip, J., et al. (2013). Leaf
326 area index estimation in vineyards using a ground-based LiDAR scanner. *Precision
327 Agriculture, 14*, 290-306.

328 Drissi, R., Goutouly, J. P., Forget, D., & Gaudillère, J. P. (2009). Nondestructive
329 measurement of grapevine leaf area by ground Normalized Difference Vegetation
330 Index. *Agronomy Journal, 101*(1), 226-231.

331 Gil, E., Escolà, A., Rosell, J. R., Planas, S., & Val, L. (2007). Variable rate application
332 of plant protection products in vineyard using ultrasonic sensors. *Crop Protection*,
333 26(8), 1287-1297.

334 Goutouly, J. P., Drissi, R., Forget, D., & Gaudillère, J. P. (2006). Characterization of
335 vine vigour by ground based NDVI measurements. In *Proceedings of the VI*
336 *International Terroir Congress* (pp. 237-241). Bordeaux, France.

337 Johnson, L. F., & Pierce, L. L. (2004). Indirect measurements of leaf area index in
338 California north coast vineyards. *HortScience*, 39(2), 236-238.

339 Johnson, L. F., Roczen, D. E., Youkhana, S. K., Nemani, R. R., & Bosch, D. F. (2003).
340 Mapping vineyard leaf area with multispectral satellite imagery. *Computers and*
341 *Electronics in Agriculture*, 38(1), 33-44.

342 Jonckheere, I., Fleck, S., Nackaerts, K., Muys, B., Coppin, P., Weiss, M., et al. (2004).
343 Review of methods for in situ leaf area index determination: Part I. Theories, sensors,
344 and hemispherical photography. *Agricultural and Forest Meteorology*, 121 (1-2), 19-35.

345 Lee, K. H., & Ehsani, R. (2009). A laser scanner based measurement system for
346 quantification of citrus tree geometric characteristics. *Applied Engineering in*
347 *Agriculture*, 25(5), 777-788.

348 Llorens, J., Gil, E., Llop, J., & Escolà, A. (2011). Ultrasonic and LIDAR sensors for
349 electronic canopy characterization in vineyards: advances to improve pesticide
350 application methods. *Sensors*, 11(2), 2177-2194.

351 López-Lozano, R., Baret, F., García de Cortázar-Atauri, I., Bertrand, N., & Casterad, M.
352 A. (2009). Optimal geometric configuration and algorithms for LAI indirect estimates
353 under row canopies: The case of vineyards. *Agricultural and Forest Meteorology*,
354 149(8), 1307-1316.

355 Mazzetto, F., Calcante, A., Mena, A., & Vercesi, A. (2010). Integration of optical and
356 analogue sensors for monitoring canopy health and vigour in precision agriculture.
357 *Precision Agriculture*, 11(6), 636-649.

358 Meier, U. (2001). Growth stages of mono-and dicotyledonous plants. BBCH
359 Monograph, 2nd Edition, Federal Biological Research Centre for Agriculture and
360 Forestry, p. 158.

361 Rosell, J. R., Sanz, R., Llorens, J., Arnó, J., Escolà, A., Ribes-Dasi, M., et al. (2009). A
362 tractor-mounted scanning LiDAR for the non-destructive measurement of vegetative
363 volume and surface area of tree-row plantations: A comparison with conventional
364 destructive measurements. *Biosystems Engineering*, 102(2), 128-134.

365 Sanz, R., Llorens, J., Escolà, A., Arnó, J., Ribes-Dasi, M., Masip, J., et al. (2011).
366 Innovative LiDAR 3D dynamic measurement system to estimate fruit-tree leaf area.
367 *Sensors*, 11(6), 5769-5791.

368 Stamatiadis, S., Taskos, D., Tsadila, E., Christofides, C., Tsadilas, C., & Schepers, J. S.
369 (2010). Comparison of passive and active canopy sensors for the estimation of vine
370 biomass production. *Precision Agriculture*, 11(3), 306-315.

371 Walklate, P. J., Cross, J. V., Richardson, G. M., Murray, R. A., & Baker, D. E. (2002).
372 Comparison of different spray volume deposition models using LIDAR measurements
373 of apple orchards. *Biosystems Engineering*, 82(3), 253-267.

374

375

376

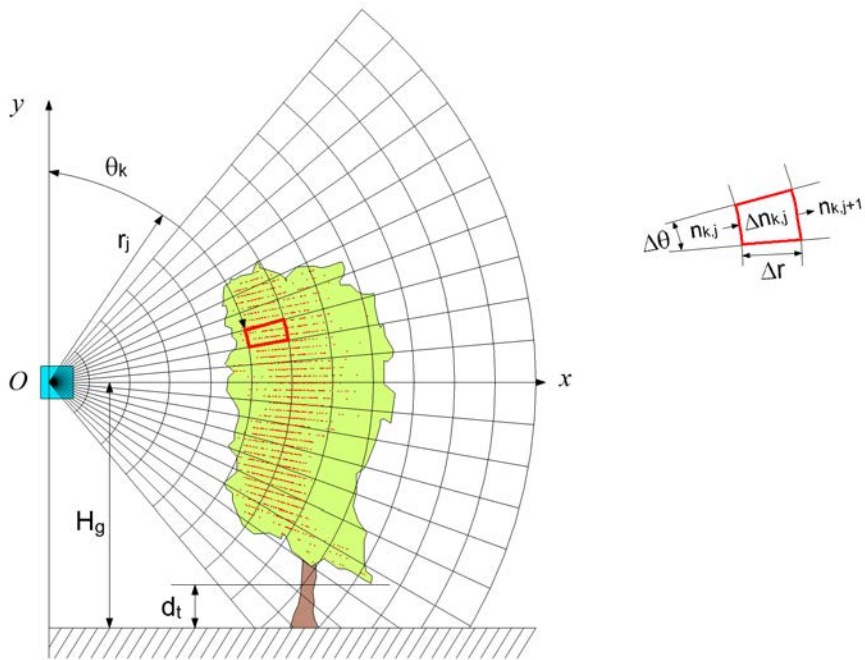
377

378

379

380

381



382

383

384

385

386

387

388

389

390

391

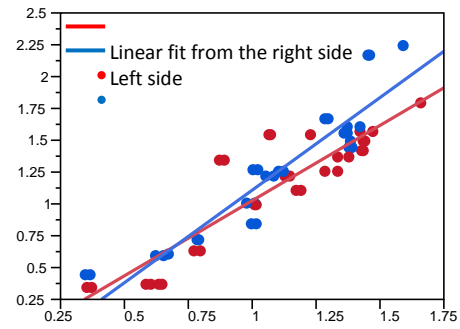
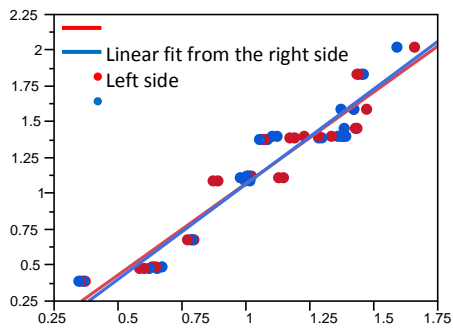
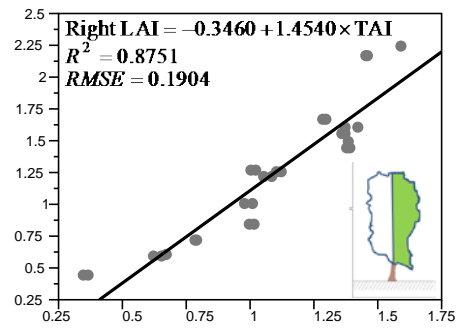
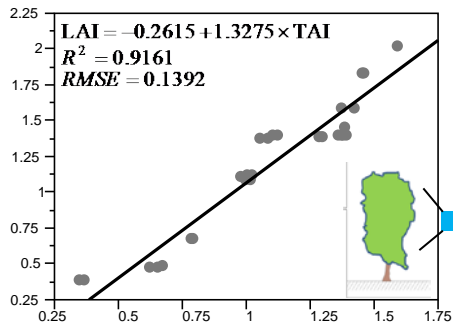
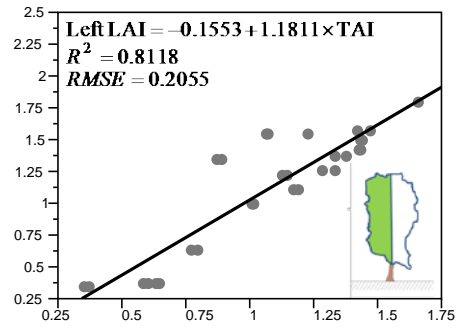
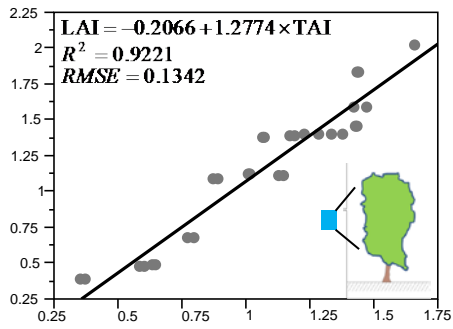
392

393

394

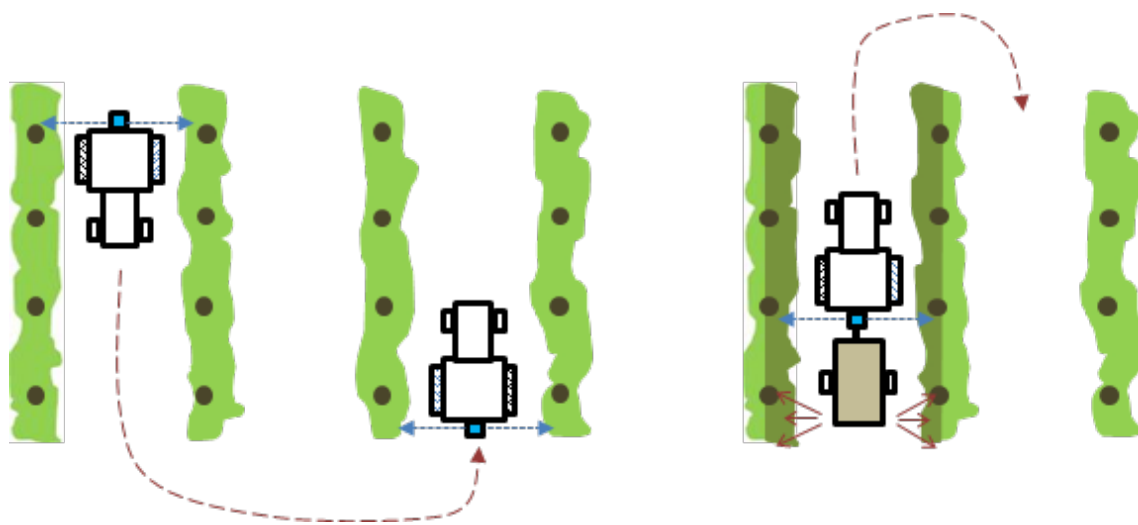
395

396



407

408



409

410